SPACE-CHARGE DOMINATED PHOTOEMISSION IN HIGH GRADIENT PHOTOCATHODE RF GUNS

Y. Chen[*a], P. Boonpornprasert[a], H. Chen[b], H. De Gersem[c], M. Dohlus[d], Y. C. Du[†b], E. Gjonaj[c],
J. D. Good[a], M. Gross[a], W. H. Huang[b], H. Huck[a], I. Isaev[a], D. Kalantaryan[a], C. Koschitzki[a],
M. Krasilnikov[‡a], O. Lishilin[a], G. Loisch[a], D. Melkumyan[a], R. Niemczyk[a], A. Oppelt[a],
H. J. Qian[§a], Y. Renier[a], S. Schmid[c], F. Stephan[a], C. X. Tang[b], Q. L. Tian[b], L. X. Yan[b]
[a]·DESY, 15738 Zeuthen, Germany; [b]·Tsinghua University, 100084 Beijing, China
[c]·TEMF, 64289 Darmstadt, Germany; [d]·DESY, 22607 Hamburg, Germany

Abstract

The cathode emission physics plays a crucial role in the overall beam dynamics in an RF gun. Interplays between intricate emission mechanisms in the cathode vicinity strongly influence the cathode quantum efficiency (QE) and the intrinsic emittance. The presence of strong space-charge effects in high gradient RF guns further complicates the emission process. A proper modeling of photoemission and a careful treatment of the space-charge contribution is thus of great necessity to understanding the formation of the beam slice emittance. In this article, emission measurements are carried out using the L-band cesium-telluride photocathode RF gun at the Photo Injector Test Facility at DESY in Zeuthen (PITZ) and the S-band copper photocathode RF gun at Tsinghua University. Following the Dowell model a simple so-called space-charge iteration approach is developed and used to determine the QE through temporal- and spatial-dependent electromagnetic fields. An impact of the space-charge cooling on the intrinsic emittance is presented. Measurement data are shown and discussed in comparisons to preliminary simulation results.

INTRODUCTION

High gradient photocathode RF guns provide high brightness electron beams for coherent light sources [1–3]. Such applications require rather high bunch charge and very small transverse normalized emittance from the injector. Optimization of the injector performance to fulfill the beam requirements is essentially a trade-off between multiple machine operation parameters. Experimental results at PITZ [2, 4, 5] have revealed optimum injector parameters from which the space-charge dominated photoemission at the cathode is identified. A detailed understanding of the contribution of the strong space-charge effects present in the cathode vicinity onto the emission process is, therefore, a prerequisite to characterize crucial beam properties at extraction, such as the thermal emittance which occupies a major part of the overall emittance budget [6].

In this article, the photoemission characterization is performed at two gun facilities, the L-band cesium-telluride photocathode RF gun at PITZ whose copies are in use at

the European XFEL and FLASH, and the S-band copper photocathode RF gun at Tsinghua University [3, 7] which has been used, for example, as the electron source for the compact Tsinghua Thomson Scattering X-ray Source [8] and many other research programs [9].

BEAM DYNAMICS

Figure 1 shows the extracted bunch charge (Q) from a cesium-telluride photocathode in the PITZ gun scanned over the full range of the emission phase (ϕ) and the applied cathode drive UV laser pulse energy (E_{las}). An 11 ps (FWHM) temporal Gaussian laser pulse with a transverse spot size of 1.2 mm in diameter is used for these measurements. The gun is operated at a maximum electric field gradient of 60 MV/m. The zero-crossing phase is at about 45°. The maximum mean momentum gain (MMMG) phase is at 6°. The charge is collected with a Faraday cup which is 0.78 m downstream of the cathode. The so-called Schottky scans (Q vs. ϕ) using different laser pulse energies and the emission curves (Q vs. E_{las}) at various RF phases are also shown in the 2D projections. In the Schottky scans, the increase of the bunch charge around 45° essentially relates to the pulse shape of the drive laser and the sharpness of the rising edge is limited by the space-charge effects as the laser pulse energy is increased. The slow increase of the charge in the middle of these curves reveals the Schottky-like effect. For the emission phases far away from the MMMG, a major part of the emitted electrons gets lost during beam transportation due to strong RF phase slippage (see [5, 10] for more details).
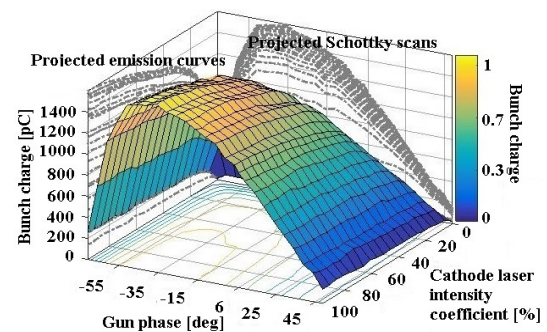

Figure 1: 3D reconstruction of a characterized photoemission distribution obtained from the experiments at PITZ. Note that the laser pulse energy is represented by the laser intensity coefficient following a linear correlation.

---

* ye.lining.chen@desy.de
† dych@mail.tsinghua.edu.cn
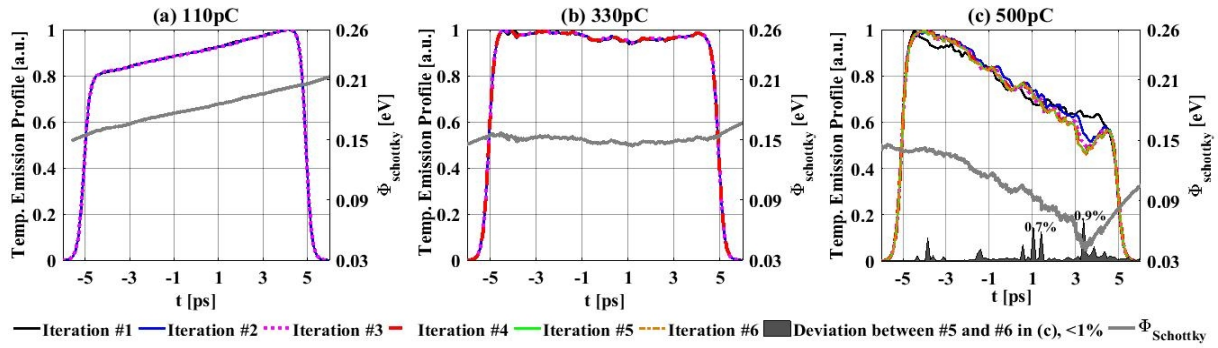‡ mikhail.krasilnikov@desy.de
§ houjun.qian@desy.de

Figure 2: Demonstration of temporal emission profile correction due to a space-charge dependent cathode work function in numerical simulations.

PHOTOEMISSION MODEL

A dispersive QE formulism is developed by David H. Dowell and John F. Schmerge [11] for metal cathodes using the Fermi-Dirac model, which reads

$$QE(\omega) = \frac{\alpha(\hbar\omega - \Phi_{\text{eff}})^2}{8\Phi_{\text{eff}}(E_F + \Phi_{\text{eff}})} \quad (1)$$

with Φ_{eff}, $\hbar\omega$, E_F and α denote the effective cathode work function, the photon energy, the Fermi energy and the form factor for characterizing the material properties, respectively. The effective work function can be written as $\Phi_{\text{eff}} = \Phi_0 \pm \Phi_{\text{schottky}} + \Phi_p$, where Φ_0 represents the intrinsic cathode work function, the terms Φ_{schottky} and Φ_p refer to the modifications of Φ_0 due to the Schottky effect and the so-called plasma layer shielding effect [12], respectively. The term Φ_p is resulted from the formation of an effective charge layer in close to cathode vicinity at very high laser intensities which shields the electrons from further emission. This results in an effective increase of the cathode work function. We model these nonlinear effects by introducing $\Phi_p(r_\perp,t) = kI^m(r_\perp,t)$ and $\Phi_{\text{schottky}}(r_\perp,t) = e\sqrt{e[E_{\text{rf}}(r_\perp,t,z=0) + E_{\text{sc}}(r_\perp,t,z=0)]/4\pi\epsilon_0}$. The symbols I, E_{rf} and E_{sc} stand for the spatial and temporal dependent parameters: the cathode drive laser intensity, the RF and space-charge fields at the cathode position, respectively. The terms k and m are fitting parameters to the experimental data. The symbol "±" in Φ_{eff} marks the moment when the full field changes its sign at $z = 0$ which refers to the cathode position.

SPACE-CHARGE DEPENDENT CATHODE WORK FUNCTION

Accurate modeling of strong space-charge effects puts a big challenge to numerical convergence of the existing space-charge tracking algorithms. To take into account the space-charge contribution to the cathode work function more properly, and therefore, to the QE, a treatment of this issue is proposed by introducing a simple "space-charge iteration approach" based on Eq. (1). The algorithm takes the emitted bunch charge produced by the drive laser following a linear run of the measured emission curve, and iteratively injects the bunch at the cathode for particle dynamics simulations from which the full fields at the cathode position are obtained. Given the fields and the prior known cathode drive laser distribution, a temporal- and spatial-dependent QE profile can be consistently determined in the iterative approach until the relative change of the temporal emission profiles between two subsequent iterations is below numerical tolerance (e.g., roughly 1% in Fig. 2 (c)). Note also that the realistic transverse emission map (see next section) is used for the modification of the transverse beam distribution while the temporal emission profile is being modulated. An in-house developed MATLAB code is used for the simulation.

In Fig. 2, simulation results of normalized temporal emission profiles and the Schottky work functions are shown for three bunch charges. The symbol "#" in the bottom legend of Fig. 2 gives the sequential number of the iteration. Note, in addition, that the smoothness of the temporal emission profiles shown here can be improved by refining the numerical parameters (e.g., number of macro-particles), and that only the longitudinal fields are considered for these simulations at the moment. Figure 4 shows the improved agreements of simulation predictions (orange and blue curves) with the measurement data (black curves) in comparison to the conventional beam dynamics simulations (dashed and dotted gray curves). The deviations in bunch charge are below 50 pC for both cases.

CHARACTERISTIC EMISSION CURVES

The space-charge iteration approach is applied to simulate the characteristic emission curves measured with a copper photocathode at Tsinghua University. The experimental conditions are summarized in Table 1. The measured transverse laser intensity distribution is shown in Fig. 3. The transverse emission map is the convolution of the QE map with the transverse distribution of the laser intensity. In our simulations, the measured laser intensity distribution is used to produce the emission map assuming a transverse homogeneous QE. All machine parameters used in the experiments are then directly plugged into the simulations for the comparison with the measurement data.

Beam dynamics, extreme beams, sources and beam related technologies

Electron and ion sources, guns, photo injectors, charge breeders

Table 1: Machine Parameters

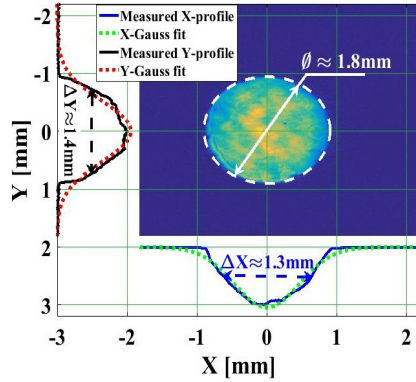| Parameters	Values
Diameter of emission area	1.8 mm
Trans. cathode laser distri.	shown in Figure 3
Cathode laser pulse energy	18–131 μJ
Temp. cathode laser distri.	flattop, 0.5/10\0.5 ps
Max. RF E-field gradient	108 MV/m
RF phase w.r.t. zero crossing	30° and 22°

Figure 3: Measured transverse intensity distribution of the cathode drive laser spot.

The saturation charge level is of interest for determining the maximum cathode beam brightness. In the cases presented in this section, the length that the electron beam extends into the vacuum by the end of the laser pulse is estimated using a cathode-anode gap model as $\Delta z \approx \frac{eE_0}{2m}\Delta t^2$ [13], where E_0 refers to the gun field applied at the cathode and Δt denotes the laser pulse duration. Compared to the radius of the transverse emission area, the length Δz is much shorter. A pancake aspect ratio of the beam is thus defined. This leads to the appliance of the "pancake emission model" in which the maximum extractable charge is simply predicted according to the maximum allowed surface charge density as $Q_{\text{sat}} \approx \epsilon_0 E_0 \pi R^2$. As shown in Fig. 4, the predicted saturation charge levels (green lines) are in good agreements with the simulated and measured ones.
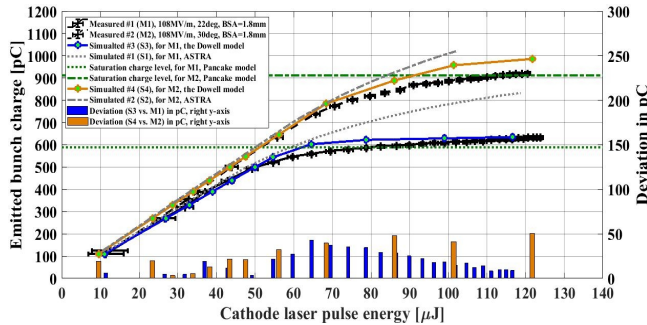

Figure 4: Characteristic emission curves: measurement vs. simulation. The terms k and m for determining Φ_p in the overall work function are estimated as 0.1 and 0.35, respectively. The ASTRA code is used for particle tracking [14].

where σ_x represents the rms beam size while the square root stands for the rms of the dimensionless transverse momen-

INTRINSIC EMITTANCE

The intrinsic emittance for metals is derived in [11] as

$$\epsilon_n = \sigma_x \sqrt{\frac{\hbar\omega - \Phi_{\text{eff}}}{3mc^2}}, \qquad (2)$$

tum. As discussed in earlier sections, the effective cathode work function is time- and space-dependent according to the spatial and temporal dependent fields formulated in Eq. (1). This effect results in a transient correlation of the sliced intrinsic emittance on the cathode surface with the emission time clock. Figure 5 shows this (surface) thermal emittance evolution during emission for variable bunch charges. The inset gives the averaged emittance as a function of the bunch charge. Higher extracted bunch charge corresponds to lower averaged beam intrinsic emittance on the cathode surface and vise versa (dotted lines). This is due to the fact that higher space-charge fields cancel out more applied acceleration fields at the cathode leading to an increased cathode work function, and therefore, a lower thermal emittance. This means, the space-charge cools down the thermal emittance, which, in fact, may partially explain why the optimum operation condition for the overall minimized transverse emittance at PITZ always results in a space-charge dominated emission at beam extraction, since the thermal emittance is one of the major parts of the optimized transverse beam emittance.
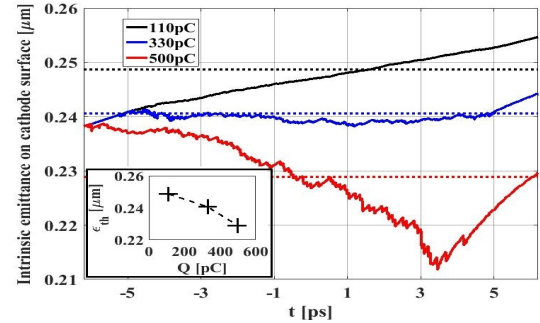

Figure 5: Space-charge influenced transient thermal emittance on the cathode surface for different bunch charges.

SUMMARY

The photoemission mechanism and the associated beam dynamics are discussed with a focus on the space-charge dominated regime. Space-charge contributions to the cathode work function are modeled through the Schottky-effect. A photoemission model is then used to link the modified cathode work function to the modulated QE. Based on a proposed space-charge iteration approach, a time- and space-dependent QE results and a transient beam intrinsic emittance on the cathode surface is obtained. A space-charge cooling effect is presented which can be potentially used for improving the overall beam emittance by reducing the thermal emittance through the extraction of multiple bunch charges. Beam dynamics simulation results show good agreements with the characteristic emission measurement data with a copper cathode at Tsinghua University. More

detailed analysis and modeling work will be presented in the near future.

REFERENCES

[1] F. Stephan and M. Krasilnikov, "High Brightness Photo Injectors for Brilliant Light Sources", in *Chapter of the book "Synchrotron Light Sources and Free-Electron Lasers"*, editors E. Jaeschke, S. Khan, J.R. Schneider, J.B. Hastings, Springer International Publishing Switzerland, ISBN 978-3-319-04507-8, 2016.

[2] M. Krasilnikov *et al.*, "Experimentally minimized beam emittance from an L-band photoinjector", *Phys. Rev. ST Accel. Beams*, vol. 15, 100701, 2012.

[3] C. X. Tang *et al.*, "Low Emittance and High Current Electron Linac Development at Tsinghua University", in *Proc. LINAC'16*, East Lansing, MI, USA, Sep. 2016, pp. 17–21. `doi:10.18429/JACoW-LINAC2016-MO2A04`

[4] Y. Chen *et al.*, "Modeling and simulation of RF photoinjectors for coherent light sources", *NIM A*, vol. 889, pp. 129–137, 2018.

[5] Y. Chen *et al.*, "Investigations of the Space-Charge-Limited Emission in the L-Band E-XFEL Photoinjector at DESY-PITZ", in *Proc. IPAC'15*, Richmond, VA, USA, May 2015, pp. 162–164. `doi:10.18429/JACoW-IPAC2015-MOPWA029`

[6] V. Miltchev *et al.*, "Transverse Emittance Measurements at the Photo Injector Test Facility at DESY Zeuthen in *Proc. FEL'04*, Trieste, Italy, Sep. 2004, paper TUPOS09, pp. 399.

[7] H. J. Qian *et al.*, "Rf Design and High Power Tests of a New Tsinghua Photocathode Rf Gun", in *Proc. FEL'12*, Nara, Japan, Aug. 2012, paper MOPD55, pp. 165–167.

[8] Y. C. Du *et al.*, "Generation of first hard X-ray pulse at Tsinghua Thomson Scattering X-ray Source", *Rev. Sci. Instrum.*, vol. 84, p. 053301, 2013.

[9] H. J. Qian *et al.*, "Experimental investigation of thermal emittance components of copper photocathode", *Phys. Rev. ST Accel. Beams*, vol. 15, p. 040102, 2012.

[10] Y. Chen *et al.*, "3d Full Electromagnetic Beam Dynamics Simulations of the PITZ Photoinjector", in *Proc. IPAC'14*, Dresden, Germany, June 2014, pp. 391–393. `doi:10.18429/JACoW-IPAC2014-MOPME008`

[11] David H. Dowell *et al.*, "Quantum efficiency and thermal emittance of metal photocathodes", *Phys. Rev. ST Accel. Beams*, vol. 12, p. 074201, 2009.

[12] Max Zolotorev, "Nonlinear effects in photocathodes", Tech. Rep., SLAC-PUB-5896, 1992.

[13] D. Filippetto *et al.*, "Maximum current density and beam brightness achievable by laser-driven electron sources", *Phys. Rev. ST Accel. Beams*, vol. 17, p. 024201, 2014.

[14] K. Floettmann, A Space Charge Tracking Algorithm (ASTRA), http://www.desy.de/ mpyflo/.